X-BAND FERROELECTRIC-ON-SI FIN BULK ACOUSTIC RESONATORS (FOS-FINBAR) WITH *f.Q* OF 0.8×10^{13}

Faysal Hakim and Roozbeh Tabrizian
Department of Electrical and Computer Engineering, University of Florida, USA

ABSTRACT

This abstract reports on ferroelectric-on-Si fin bulk acoustic resonators (FoS-FinBAR) operating at ~X-band with large quality factors (Q) as high as 1032, and a record-high frequency-Q product (f×Q) nearing 10^{13}. This high performance is achieved through a novel fabrication process that enables perfect control over the three-dimensional geometry of the device and its transducer electrodes, as well as crystalline quality of the constituent materials. The process is based on (a) crystallographic-orientation-dependent etching of Si micro-fins with perfectly straight sidewall and aspect ratio exceeding 20:1, (b) conformal atomic-layer-deposition of sidewall ferroelectric transducers, and (c) three-dimensional patterning of transducer electrodes. FoS-FinBARs with a fin width of 1.2µm and hafnia-zirconia transducer of 50nm thickness are presented. The devices are operating in 3rd width-extensional bulk acoustic mode at 7.75 and 7.78 GHz, with Qs of 961 and 1032, and electromechanical coupling (k_t^2) of 1.29% and 0.89%, respectively. The large f×Q of 0.8×10^{13} at ~8 GHz, solidly-mounted structure, lithographical frequency scalability, and the CMOS-compatible fabrication process of the X-band FoS-FinBARs highlight their potential to realize multi-frequency and monolithically integrated oscillators and channel-select filters.

KEYWORDS

Ferroelectric, Hafnia-Zirconia, Fin Bulk Acoustic Resonator (FinBAR), X-band, Three-dimensional Patterning, Sidewall Transducer, High Q, CMOS Compatible.

INTRODUCTION

Current wireless spectrum resource, extending from 0.3 to 6 GHz, is on the verge of congestion due to exponential increase in the number of users introduced by internet of things, and the emergence of broadband applications such as metaverse. To address the grand challenge of spectrum limitation, new wireless technologies aim to use spread-spectrum techniques based on reconfiguration over numerous bands, and also extension to operate in untapped spectrum in cm- and mm-wave regimes [1]. These goals, however, are currently intangible, due to the fundamental limitations of available frequency control technologies.

The frequency control in existing wireless systems is indispensably dependent on piezoelectric bulk acoustic wave (BAW) resonator technologies to realize RF filters and oscillators for front-end modules. Current piezoelectric BAW resonators, created in aluminum nitride (AlN) films and operating in thickness mode, are fundamentally incapable to realize spread-spectrum frequency generation and control for modern wireless systems operating in super- and extremely-high-frequency regimes. This is primarily due to their limited lithographic frequency scaling and large area that prevents single-chip multi-band integration and impose large footprint consumption. Further, the k_t^2 and Q of these resonators significantly drop at higher frequencies, due to significant degradation of sputtered AlN quality at lower thicknesses required for frequency scaling [2-4]. To overcome these limitations, new technologies are developed based on alternative materials (*e.g.*, lithium niobate, scandium-aluminum nitride) and high-order modes [5-9]. However, these approaches do not provide transforming solution, since they still rely on planar architectures and inherit similar limitations of AlN BAW, although incrementally relieve frequency and integration limits.

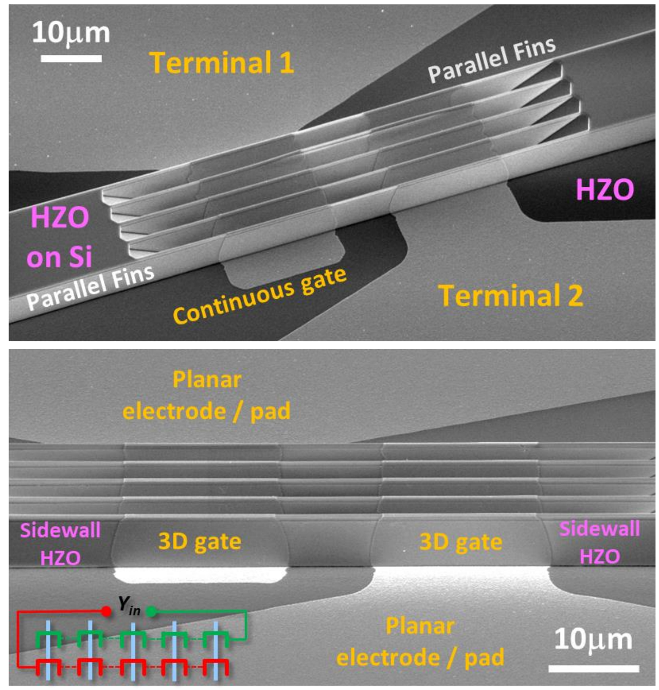

Figure 1: SEM images of multi-gate HZO-on-Si FinBAR, highlighting the fins, 3D-patterend gates and planar pads. The inset shows the connection of gates to form two terminals.

An alternative three-dimensional fin bulk acoustic resonator (FinBAR) technology has been developed in this regard that operates on excitation of bulk acoustic modes in high aspect-ratio semiconductor fins [10-12]. Benefiting from the width variation and single-crystallinity of fins, this technology offers multitude advantages over planar counterparts such as extreme lithographical frequency scalability, high Q, improved power handling and linearity, and an order of magnitude smaller footprint [13]. Realizing FinBARs however requires addressing major manufacturing challenges including growth of textured piezoelectric films and low-loss metal electrodes on the sidewall, and definition of high-aspect ratio fins with minimum width variation across the height. These features are essential to achieve high k_t^2 and Q width-extensional resonance modes in FinBARs.

In this work, we present a new generation of ferroelectric-on-silicon (FoS) FinBARs based on a novel fabrication process that creates mirror smooth and perfectly straight fin profile, high quality sidewall piezoelectric films, and three-dimensional patterning of low-loss electrodes / gates on the sidewall of the fins. Proof of concept devices are presented at 8 GHz, based on 1.2µm-wide Si fin, 50nm-thick hafnia-zirconia (HZO) sidewall piezoelectric transducer, and atomic-layer-deposited tungsten (W) gates, showing a record-high f×Q of ~0.8×10^{13}. Figure 1 shows the scanning electron microscope (SEM) images of fabricated FoS-FinBAR from different angles, highlighting the ideal geometry of fins, 3D-patterened gates, and arraying scheme used to increase transduction area and reduce admittance.

FOS-FINBAR DESIGN AND MODELING

FoS-FinBAR is modeled using Mason's waveguide-based approach [14], to identify the resonance frequency, Q and k_t^2 based on the transducer and electrode thicknesses, fin width, and fundamental material properties. Figure 2 (a) shows the model created from cascading acoustic waveguides that represent metal electrode, HZO piezoelectric film, and Si fin. The model represents two W-HZO-W sidewall transducers that are placed on the two ends of the Si fin. Each waveguide, created from a lossy elastic medium with a wavenumber k, is modeled with series (Z_s) and shunt (Z_p) impedances in T-shaped network where:

$$\begin{aligned} Z_s &= jZ\tan\left(\frac{kd}{2}\right), \\ Z_p &= -jZ/\sin(kd) \end{aligned} \qquad (1).$$

Here, $k = \frac{2\pi f d}{v}\left(1-\frac{j}{2Q_m}\right)$, and d, Z, v, and Q_m are layer thickness, acoustic impedance, longitudinal acoustic velocity, and material quality factor, respectively. Besides, the equivalent waveguide model of the piezoelectric layer includes a lossy static capacitor (C_0) and a transformer with efficiency (η) defined by longitudinal piezoelectric coefficient (e_{33}), defined as:

$$\begin{aligned} C_0 &= \frac{\varepsilon A}{d}, \\ \eta &= e_{33}\frac{C_0}{\varepsilon} \end{aligned} \qquad (2),$$

where, A is the sidewall transduction area and ε is the dielectric constant of the piezoelectric film. Figure 2 (b) shows the admittance of the FoS-FinBARs operating in 3rd width-extensional modes. The resonators are modeled with 50nm HZO sidewall transducer sandwiched between 30nm W electrodes, and based on using different Si fin widths, to highlight the lithographical frequency scalability of FoS-FinBARs.

When targeting for a particular resonance frequency value, the transducer stack thickness and fin width can be tailored to achieve the desirable k_t^2 and Q. Figure 3 shows the simulated (using Mason's model) Q and k_t^2 of 8 GHz FoS-FinBAR created from proper combination of transducer thickness and fin width to achieve 8 GHz resonance frequency for the 3rd width-extensional mode. Opting for narrower Si fins and thicker HZO transducer thickness results in lower Q and higher k_t^2 values. This is due to the higher fraction of electromechanically active volume of the resonator and also the higher energy dissipation in HZO film compared to single-crystal Si fin. On the other hand, opting for wider fins and thinner sidewall HZO thickness results in a Q increase and k_t^2 drop. This results in a nearly constant $k_t^2.Q$ product at any frequency, regardless of the relative thickness of HZO transducer and width of Si fin.

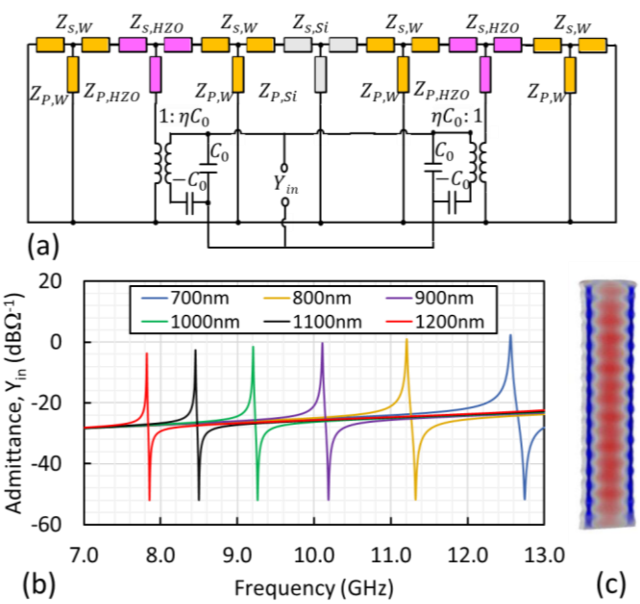

Figure 2: (a) Electrical equivalent circuit model from Mason's waveguide approach for FoS-FinBAR; (b) simulated admittance of FoS-FinBARs with different fin widths, operating in 3rd width-extensional bulk acoustic mode (WE3), highlighting lithographical frequency scalability; (c) COMSOL simulated cross-sectional mode-shape of FoS-FinBAR operating in WE3 mode.

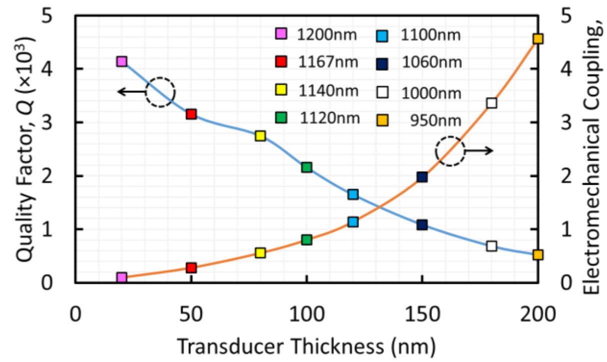

Figure 3: Simulated performance metrics (quality factor, Q on left Y-axis and electromechanical coupling, k_t^2 on right Y-axis) for 8 GHz FoS-FinBARs created from different combinations of HZO transducer thickness and fin width.

FABRICATION PROCESS

Figure 4 shows the fabrication process flow of the presented FoS-FinBAR. To achieve mirror-smooth fin sidewall with negligible width variation across height, crystallographic-orientation dependent Si etch is performed. In this process, (110)

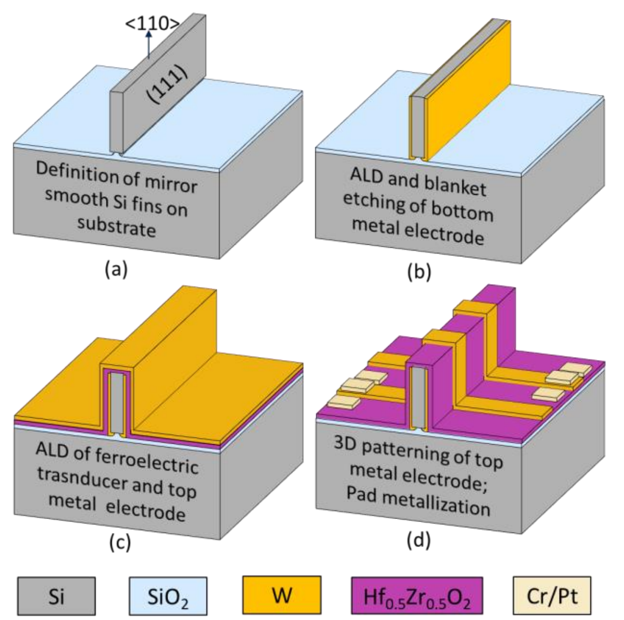

Figure 4: Three mask fabrication process flow of FoS- FinBARs: (a) wet-etching Si fins with (111)-plan etch-stop; (b) ALD and selective patterning of the first W electrode; (c) ALD of ferroelectric HZO transducer and top metal followed by crystallization annealing; (d) 3D patterning of top gates by isotropic dry etch.

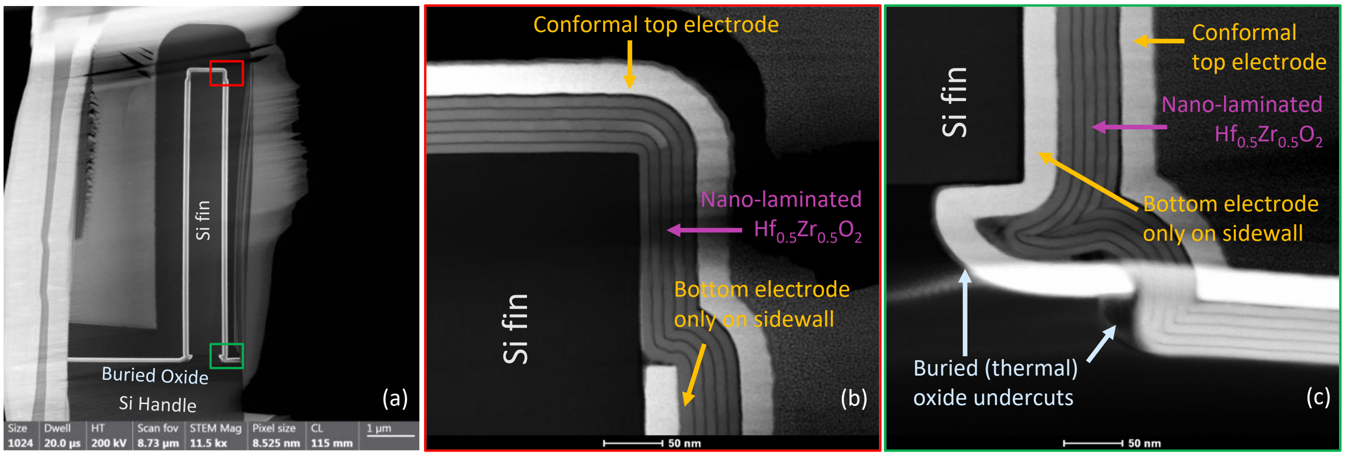

Figure 5: (a) HR-TEM image of ferroelectric-on-Si FinBAR cross-section, highlighting the high aspect ratio and perfectly straight fin sidewalls; Zoomed in HR-TEM images of (b) top and (c) bottom corners of FoS-FinBAR (red and green boxes in (a), respectively) highlighting mirror smooth sidewall, sidewall-only bottom electrode, and conformally deposited metal-ferroelectric-metal transducer stack.

oriented 6μm-thick SOI substrate is etched in 2.3% TMAH solution at 65^{O}C, using SiO_2 hard mask. The heated wet-etching enables creation of high aspect-ratio (> 20:1) Si fins with perfectly vertical sidewalls defined by (111) plane, which acts as a etch stop (Fig. 4 (a)). Once the fins are patterned, a 30nm W layer is deposited using plasma-enhanced ALD. This is followed by blanket dry-etching to remove W everywhere except the sidewall of fins (Fig. 4 (b)). Next, the nano-laminated hafnia-zirconia film, constituting of five ~10nm $Hf_{0.5}Zr_{0.5}O_2$ layers interrupted with 1nm alumina (Al_2O_3) interlayers, is deposited using ALD, and followed by crystallization in polar orthorhombic phase by rapid thermal annealing (Fig. 4 (c)). The nano-lamination is essential to scale the thickness of sidewall transducer beyond the ~20nm limit at which the morphology is transformed to non-polar, and nonpiezoelectric, tetragonal phase [15]. Next, a 30nm W layer is deposited by ALD and three-dimensionally patterned by isotropic dry-etch in SF_6 to create the top electrodes / gates (Fig. 4 (d)). Finally, 250nm thick Pt/Cr layer is deposited using lift-off to create low-loss routing and pads.

Figure 5 shows cross-sectional high-resolution transmission electron microscopy (HR-TEM) images of FoS-FinBAR. Figure 5(a) shows the high-aspect ratio FoS-FinBAR cross-section with 6μm tall and 500nm wide fins with sidewall ferroelectric transducer. Figure 5(b) and 5(c) show successful patterning of bottom electrode, as shown at top and bottom corners of the fin, highlighting the presence of bottom electrode only on sidewalls. This is essential for reduction of static feedthrough that degrade FoS-FinBAR admittance. The conformal nature of HZO film and top W gate is also evident. This conformality is essential to create arrayed fin schemes for scaling transduction area and facilitate electrical measurement of the devices using planar pads.

CHARACTERIZATION OF FOS-FINBAR

The fabricated FoS-FinBARs are measured to evaluate the ferroelectric, and hence, piezoelectric, behavior of the sidewall HZO transducer and the RF admittance. The ferroelectric behavior is measured using Radiant PiezoMEMS tester. Figure 6 (a) shows the measured polarization hysteresis loop for the FoS-FinBAR, highlighting a large remanent polarization of 23.6 μC/cm^2 with coercive field of 2.52 MV/cm, indicating properly poled transducer. The admittance of FoS-FinBARs is extracted by measuring reflection response (S_{11}) of the one-port resonator using a Keysight N5222A Vector Network Analyzer. Figure 6 (b) shows measured admittance of two identical FoS-FinBARs randomly selected across the 100mm wafer, highlighting frequencies of 7.75 GHz and 7.78 GHz, with a sub-1% offset, *Q*s of 961 and 1032, and k_t^2 of 1.29% and 0.89%, respectively.

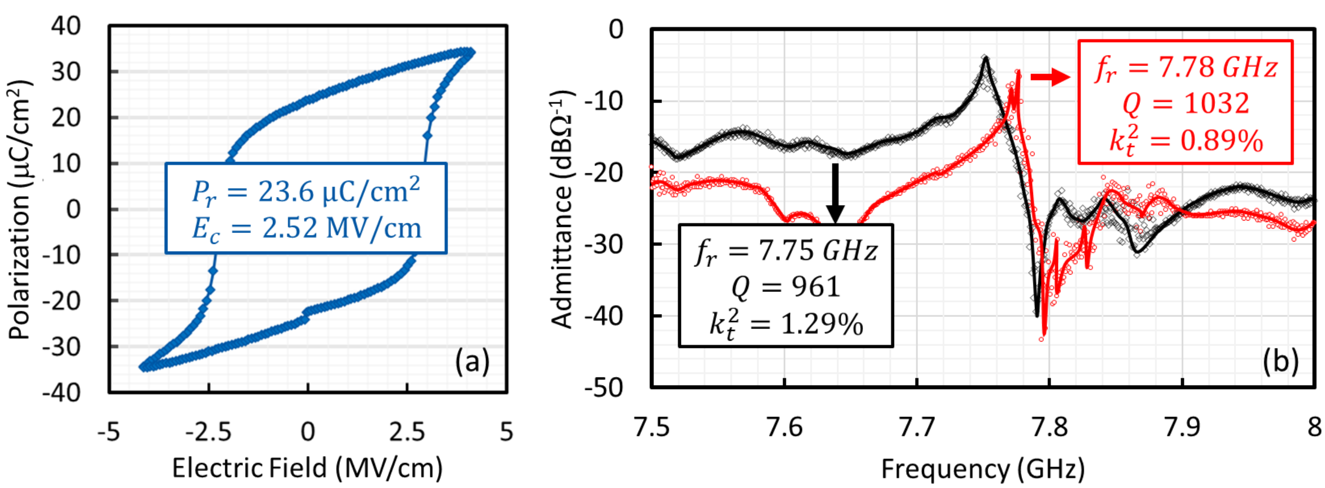

Figure 6: (a) Measured polarization-electric field hysteresis loop of FoS-FinBAR, highlighting the ferroelectricity and piezoelectricity of sidewall HZO transducer; (b) measured RF admittance of fabricated FoS-FinBARs operating at 7.75GHz and 7.78 GHz, with f.Q of 0.8×10^{13}.

CONCLUSION

This paper presents novel Ferroelectric-on-Si Fin Bulk Acoustic Resonators (FoS-FinBAR), based on the use of a novel fabrication process. The process enables creation of perfectly straight high aspect-ratio fins with mirror-smooth sidewalls, highly piezoelectric sidewall transducers based on atomic layer deposited ferroelectric hafnia-zirconia and tungsten electrodes, and three-dimensional patterning of electrodes and gates. FoS-FinBAR prototypes are presented at ~ 8 GHz with Qs as high as 1032 and k_t^2 as high as 1.3%, resulting in highest $f.Q$ product of 0.8×10^{13}. The extreme lithographical frequency scalability, CMOS-compatible materials and fabrication process, and high k_t^2 and Q, tailorable with fin width and transducer thickness, highlights the promise of FoS-FinBAR technology for realization of cm- and mm-wave integrated oscillators and filters for spread-spectrum wireless systems.

ACKNOWLEDGEMENTS

This project is supported by DARPA Young Faculty Award program. The authors would like to thank DARPA program manager Dr. Timothy Hancock for his support of this work. The authors would also like to thank the staffs at Nanoscale research facility at the University of Florida.

REFERENCES

[1] M. Matthaiou, O. Yurduseven, H. Q. Ngo, D. Morales-Jimenez, S. L. Cotton and V. F. Fusco, "The Road to 6G: Ten Physical Layer Challenges for Communications Engineers," in *IEEE Communications Magazine*, vol. 59, no. 1, pp. 64-69, January 2021, doi: 10.1109/MCOM.001.2000208.

[2] R. Aigner, G. Fattinger, M. Schaefer, K. Karnati, R. Rothemund and F. Dumont, "BAW Filters for 5G Bands," *2018 IEEE International Electron Devices Meeting (IEDM)*, San Francisco, CA, USA, 2018, pp. 14.5.1-14.5.4, doi: 10.1109/IEDM.2018.8614564.

[3] E. Iborra, M. Clement, J. Capilla, and V. Felmetsger, "Low-thickness high-quality aluminum nitride films for super high frequency solidly mounted resonators," *Thin Solid Films*, 520(7), 3060-3063, 2012.

[4] U. Zaghloul and G. Piazza, "Synthesis and characterization of 10 nm thick piezoelectric AlN films with high c-axis orientation for miniaturized nanoelectromechanical devices." *Applied Physics Letters* 104.25 (2014): 253101.

[5] Y. Yang, R. Lu, L. Gao, & S. Gong, "10–60-GHz Electromechanical Resonators Using Thin-Film Lithium Niobate". *IEEE Transactions on Microwave Theory and Techniques*, vol. 68, p. 5211-5220, 2020.

[6] M. Assylbekova, G. Chen, G. Michetti, M. Pirro, L. Colombo & M. Rinaldi, "11 GHz Lateral-Field-Excited Aluminum Nitride Cross-Sectional Lamé Mode Resonator," *In 2020 Joint Conference of the IEEE International Frequency Control Symposium and International Symposium on Applications of Ferroelectrics (IFCS-ISAF)*, p. 1-4, IEEE,2020.

[7] M. Park, Z. Hao, D. G. Kim, A. Clark, R. Dargis and A. Ansari, "A 10 GHz Single-Crystalline Scandium-Doped Aluminum Nitride Lamb-Wave Resonator," *2019 20th International Conference on Solid-State Sensors, Actuators and Microsystems & Eurosensors XXXIII (TRANSDUCERS & EUROSENSORS XXXIII)*, Berlin, Germany, 2019, pp. 450-453, doi: 10.1109/TRANSDUCERS.2019.8808374.

[8] M. Ghatge, V. Felmetsger and R. Tabrizian, "High $k_t^2.Q$ Waveguide-Based ScAlN-on-Si UHF and SHF Resonators," *2018 IEEE International Frequency Control Symposium (IFCS)*, 2018, pp. 1-4, doi: 10.1109/FCS.2018.8597447.

[9] S. Rassay, D. Mo, C. Li, N. Choudhary, C. Forgey and R. Tabrizian, "Intrinsically Switchable Ferroelectric Scandium Aluminum Nitride Lamb-Mode Resonators," in *IEEE Electron Device Letters*, vol. 42, no. 7, pp. 1065-1068, July 2021, doi: 10.1109/LED.2021.3078444.

[10] M. Ramezani, M. Ghatge and R. Tabrizian, "High-Q silicon fin bulk acoustic resonators for signal processing beyond the UHF," *2017 IEEE International Electron Devices Meeting (IEDM)*, 2017, pp. 40.1.1-40.1.4, doi: 10.1109/IEDM.2017.8268524.

[11] M. Ramezani, M. Ghatge and R. Tabrizian, "High $k_t^2.Q$ silicon Fin Bulk Acoustic Resonators (FinBAR) FOR chip-scale multi-band spectrum analysis," *2018 IEEE Micro Electro Mechanical Systems (MEMS)*, Belfast, UK, 2018, pp. 158-161, doi: 10.1109/MEMSYS.2018.8346508.

[12] M. Ramezani, M. Ghatge, V. Felmetsger and R. Tabrizian, "A Super-High-Frequency Non-Released Silicon Fin Bulk Acoustic Resonator," *2019 IEEE MTT-S International Microwave Symposium (IMS)*, Boston, MA, USA, 2019, pp. 516-519, doi: 10.1109/MWSYM.2019.8700907.

[13] F. Hakim, T. Tharpe and R. Tabrizian, "Ferroelectric-on-Si Super-High-Frequency Fin Bulk Acoustic Resonators With $Hf_{0.5}Zr_{0.5}O_2$ Nanolaminated Transducers," in *IEEE Microwave and Wireless Components Letters*, vol. 31, no. 6, pp. 701-704, June 2021, doi: 10.1109/LMWC.2021.3067509.

[14] W. P. Mason, *Physical Acoustics Principles and Methods, vol. 1A*. New York: Academic Press, 1964.

[15] S. Riedel, P. Polakowski, and J. Müller, "A thermally robust and thickness independent ferroelectric phase in laminated hafnium zirconium oxide," *AIP Advances*, vol. 6, pp. 095123, 2016.

CONTACT

*Faysal Hakim, tel: +1-352-745-9511; hakimfaysal@ufl.edu.